US 20160296202A1

(19) **United States**

(12) **Patent Application Publication** (10) **Pub. No.: US 2016/0296202 A1**

ROBERT et al. (43) **Pub. Date: Oct. 13, 2016**

(54) **BEAMFORMING TECHNIQUES FOR ULTRASOUND MICROCALCIFICATION DETECTION**

(71) Applicant: **KONINKLIJKE PHILIPS N.V.**, Eindhoven (NL)

(72) Inventors: **JEAN-LUC ROBERT**, WHITE PLAINS, NY (US); **SHENG-WEN HUANG**, OSSINING, NY (US); **EMIL GEORGE RADULESCU**, OSSINING, NY (US); **FRANCOIS GUY GERARD MARIE VIGNON**, CROTON-ON-HUDSON, NY (US); **RAMON QUIDO ERKAMP**, YORKTOWN HEIGHTS, NY (US)

(21) Appl. No.: **14/777,564**

(22) PCT Filed: **Mar. 12, 2014**

(86) PCT No.: **PCT/IB2014/059657**

§ 371 (c)(1),
(2) Date: **Sep. 16, 2015**

Related U.S. Application Data

(60) Provisional application No. 61/803,634, filed on Mar. 20, 2013, provisional application No. 61/907,022, filed on Nov. 21, 2013.

Publication Classification

(51) **Int. Cl.**
A61B 8/08 (2006.01)
A61B 8/00 (2006.01)

(52) **U.S. Cl.**
CPC ***A61B 8/085*** (2013.01); ***A61B 8/461*** (2013.01); ***A61B 8/5223*** (2013.01); ***A61B 8/0825*** (2013.01); ***A61B 8/5207*** (2013.01)

(57) **ABSTRACT**

A medical ultrasound acquisition-data analysis device acquires channel data (**144**) via ultrasound received on the channels, uses the acquired channel data to estimate data coherence and derive dominance of an eigen-value of a channel covariance matrix and, based on the estimate and dominance, distinguishes microcalcifications (**142**) from background. Microcalcifications may then be made distinguishable visually on screen via highlighting, coloring, annotation, etc. The channel data operable upon by the estimating may have been subject to beamforming delays and may be summed in a beamforming procedure executed in the estimating. In the estimating and deriving, both field point-by-field point, multiple serial transmits (116, 118) may be used for each field point. In one embodiment results of the estimating and deriving are multiplied point-by-point and submitted to thresholding.

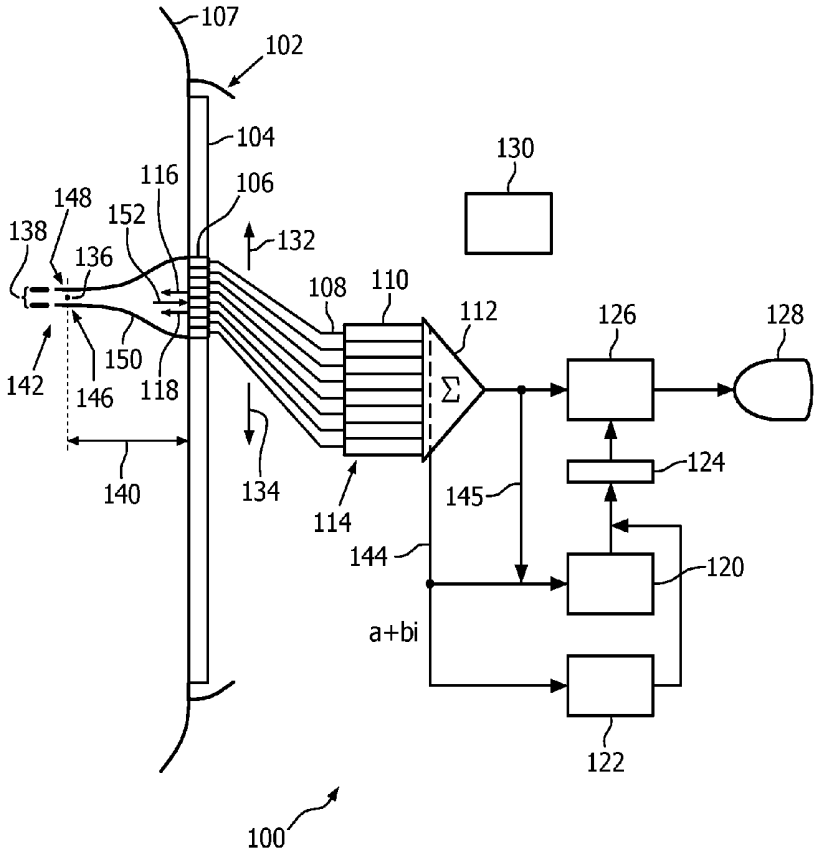

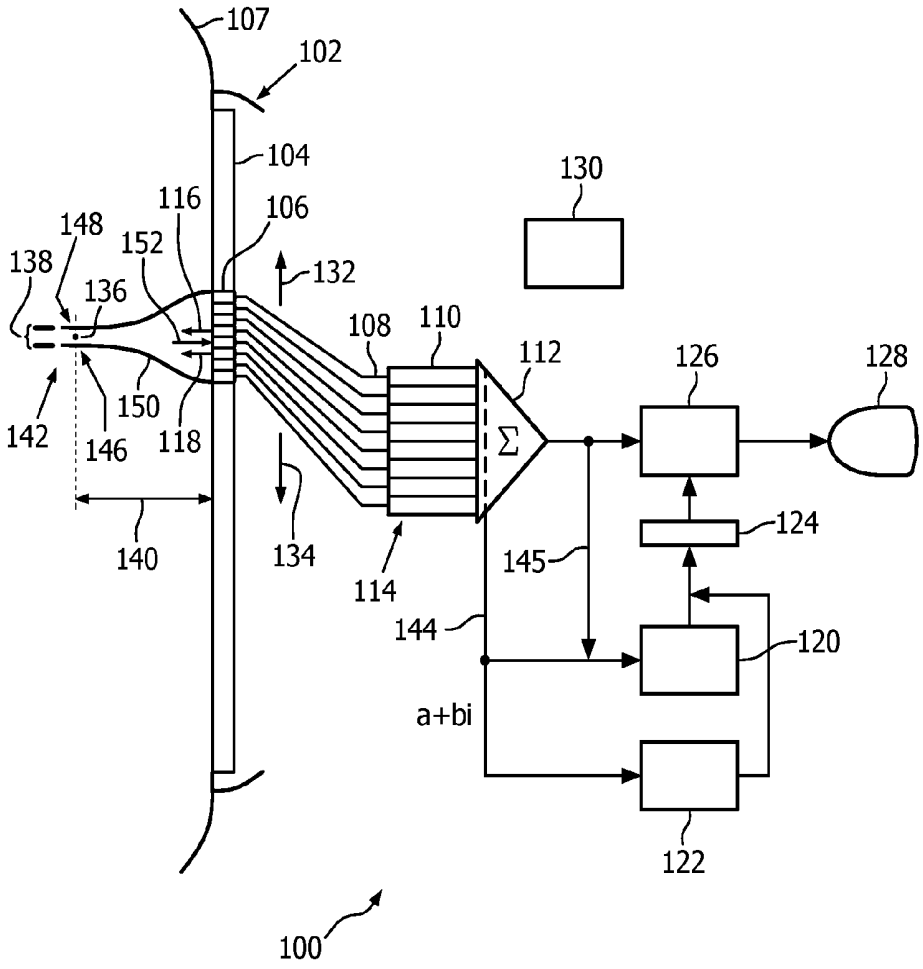
107
102
104
130
116
106
148
152
138
136
132
108
110
112
126
128
142
150
146
118
Σ
124
140
134
114
145
144
120
a+bi
122
100

FIG. 1

$$CF(m,rx) \equiv \frac{\sum_{tx=rx-\Delta}^{rx+\Delta} \left| \sum_{n=1}^{N} S(m,n,tx,rx) \right|^2}{\sum_{tx=rx-\Delta}^{rx+\Delta} N \sum_{n=1}^{N} \left| S(m,n,tx,rx) \right|^2} \quad \text{(definition 1)}$$

204, 206, 208

$$R(m,rx) \equiv \frac{1}{2d+1} \sum_{p=m-d}^{m+d} s(p,rx) s^H(p,rx) \quad \text{(definition 2)}$$

210, 214, 220, 222, 230

$$\text{where} \quad s(p,rx) = \begin{bmatrix} S(p,1,rx,rx) \\ S(p,2,rx,rx) \\ \vdots \\ S(p,N,rx,rx) \end{bmatrix} \quad \text{(definition 3)}$$

$$Tr\{R(m,rx)\} \equiv \sum_{i=1}^{N} R_{ii}(m,rx) = \sum_{i=1}^{N} \gamma_i(m,rx) \quad \text{(definition 4)}$$

212

$$ev_d(m,rx) \equiv \frac{1}{1 - \frac{\gamma_1(m,rx)}{Tr\{R(m,rx)\}}} \quad \text{(definition 5)}$$

216, 218, 228

$$R(m,rx) \equiv \frac{1}{(2d+1)(2g+1)} \sum_{p=m-d}^{m+d} \sum_{tx=rx=g}^{rx+g} s(p,tx,rx) s^H(p,tx,rx) \quad \text{(definition 6)}$$

226, 224

$$\text{where} \quad s(p,tx,rx) = \begin{bmatrix} S(p,1,tx,rx) \\ S(p,2,tx,rx) \\ \vdots \\ S(p,N,tx,rx) \end{bmatrix} \quad \text{(definition 7)}$$

FIG. 2

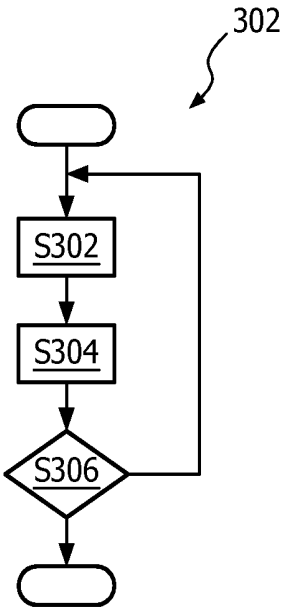

FIG. 3A

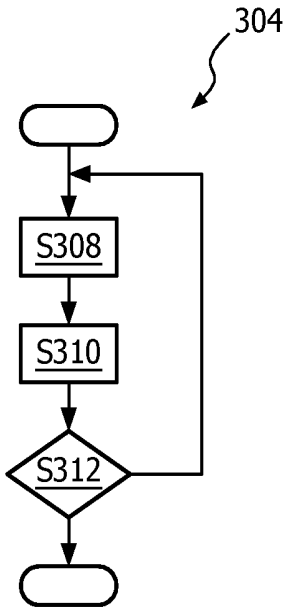

FIG. 3B

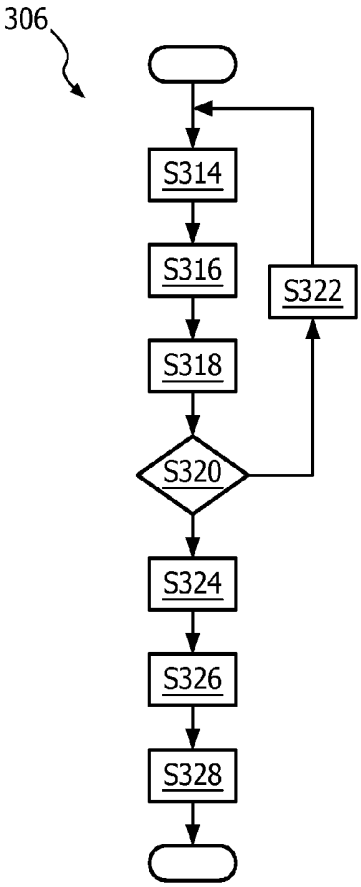
306
S314
S316
S318
S320
S322
S324
S326
S328

FIG. 3C

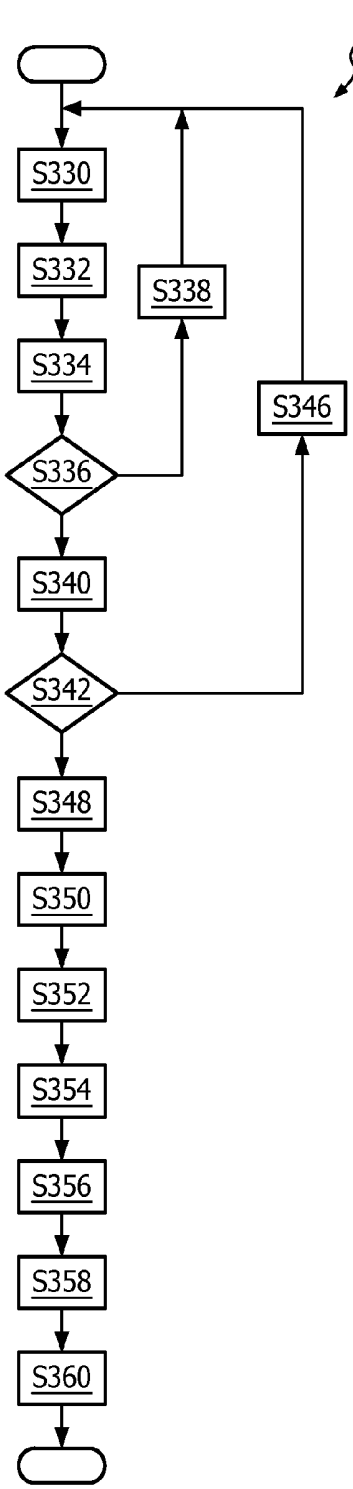
308
S330
S332
S334
S336
S338
S340
S342
S346
S348
S350
S352
S354
S356
S358
S360

FIG. 3D

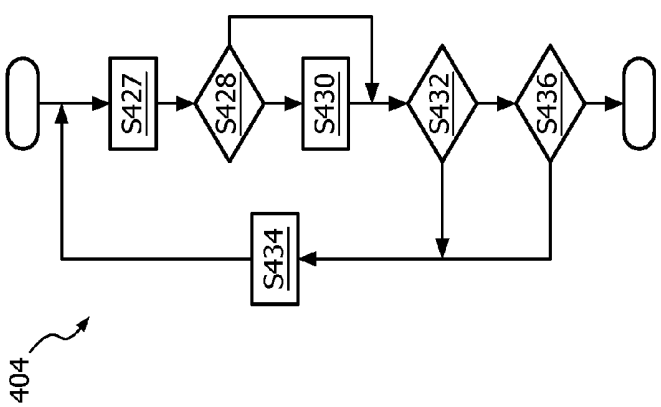
S427
S428
S430
S432
S436
S434
404

FIG. 4B

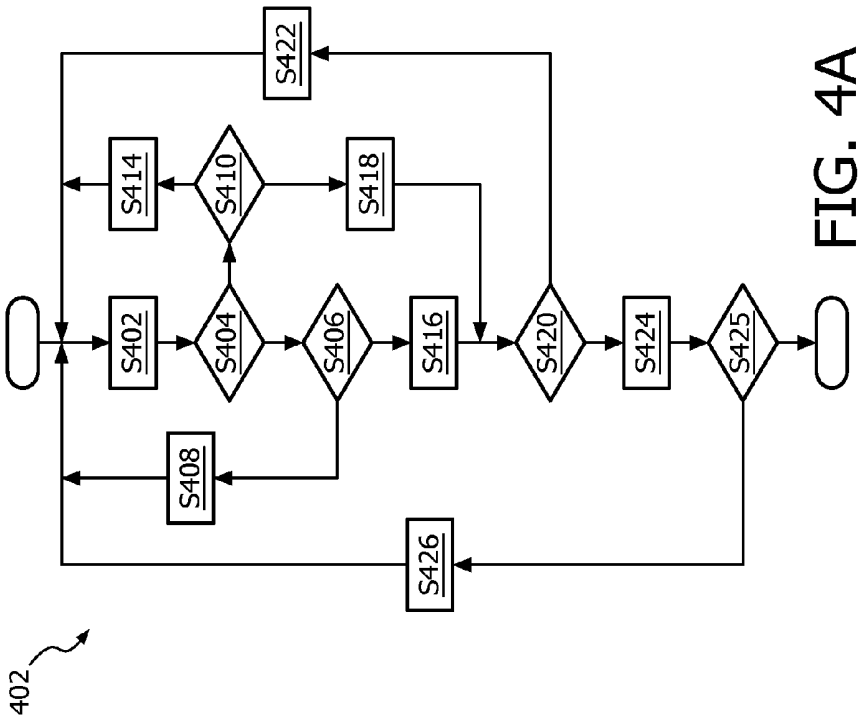
S422
S414
S410
S418
S402
S404
S406
S416
S420
S424
S425
S408
S426
402

FIG. 4A

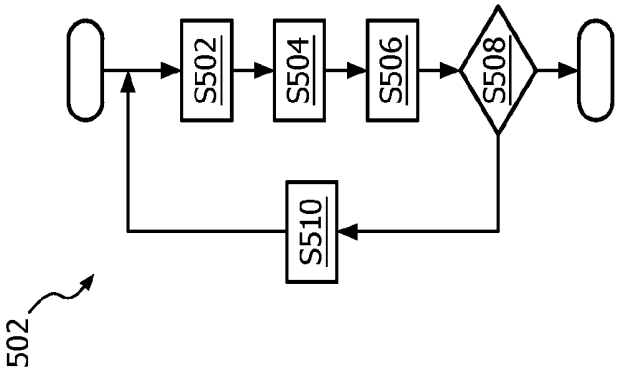
S502
S504
S506
S508
S510
502

FIG. 5

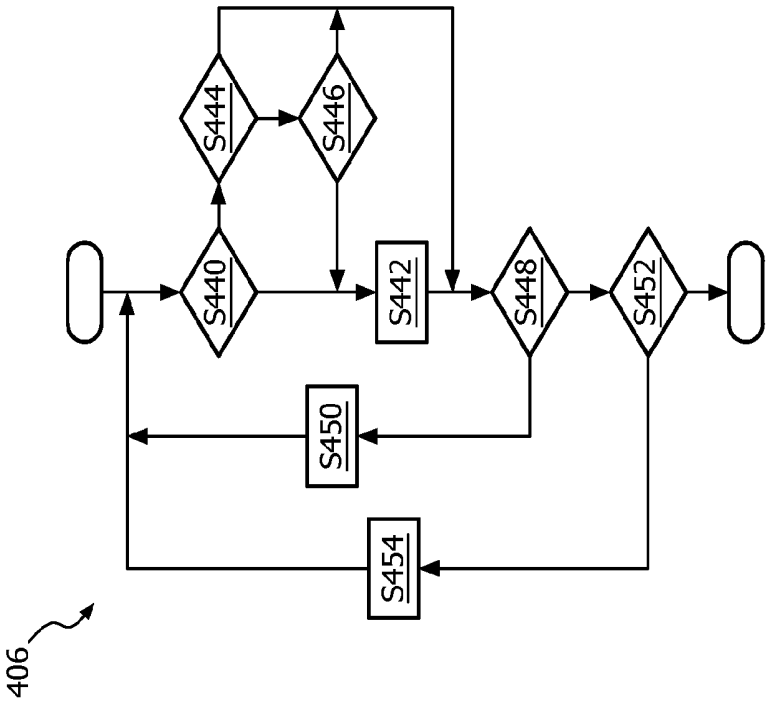
S444
S446
S440
S442
S448
S452
S450
S454
406

FIG. 4C

BEAMFORMING TECHNIQUES FOR ULTRASOUND MICROCALCIFICATION DETECTION

CROSS-REFERENCE TO PRIOR APPLICATION

[0001] This application claims the benefit of U.S. Provisional Patent Application No. 61/803,634, filed Mar. 20, 2013 and U.S. Provisional Patent Application No. 61/907,022, filed Nov. 21, 2013. These applications are hereby incorporated by reference herein.

FIELD OF THE INVENTION

[0002] The present invention relates to medical imaging for identifying microcalcifications and, more particularly, to use of ultrasound as the imaging modality.

BACKGROUND OF THE INVENTION

[0003] Mammography's success for screening for breast cancer is mostly attributed to its capability for reliably imaging calcifications, an important marker for early stage breast cancer. Microcalcifications are present in 60-80% of breast cancers and are a reliable indicator of both benign and malignant lesions. The key diagnostic features of microcalcifications are their location, number, size, morphology, distribution, pattern, and relation to a mass. These features help stratify the risk of malignancy and often are the only marker of cancer. A relevant example is Ductal Carcinoma in Situ (DCIS), which accounts for 20% of breast cancers.

[0004] However, mammography shows poor performance in dense breast tissue, the non-fatty portion of the breast. Dense breast tissue is more commonly found in younger women, and women in certain localities, China for example.

[0005] Also, despite measures to reduce the dose, mammography exposes the patient to ionizing radiation. In addition, there is the issue of patient comfort due to the need for compression plates.

[0006] The major limitation of conventional ultrasound, which is non-ionizing and needs no compression plates, is its poor sensitivity to microcalcifications. The sensitivity to microcalcifications is within 50-80%.

[0007] Mallart discloses phase aberration correction of an ultrasonic transmit beam for the inhomogeneities of a medium through the use of a receive focusing criterion that is independent of both the scattering cross-section of the medium and the transmitted energy. See R. Mallart and M. Fink, "Adaptive focusing in scattering media through sound-speed inhomogeneities: The van Cittert Zernike approach and focusing criterion," J. Acoust. Soc. Am., vol. 96, no. 6, pp. 3721-3732, 1994.

SUMMARY OF THE INVENTION

[0008] What is proposed herein below is directed to addressing one or more of the above concerns.

[0009] Channel data contain much more information than B-mode images obtained after ultrasound receive beamforming. Therefore, channel-data-based beamforming techniques can provide better sensitivity and/or specificity for microcalcification detection than image processing techniques. The novel technology proposed herein enhances the contrast between microcalcifications and the background, i.e., body tissue in which the calcifications reside, typically soft tissue such as dense breast tissue.

[0010] In addition to the advantages noted above in using ultrasound for early-stage breast cancer detection, the screening and follow-up diagnostic procedures will be greatly simplified due to medical evaluation using only one modality. Also, good sensitivity to microcalcifications will facilitate easier identification of tumor location in ultrasound-guided biopsies, improving the workflow and diagnostic confidence.

[0011] In accordance with what is proposed herein, a medical ultrasound acquisition-data analysis device having channels is configured for: acquiring channel data via ultrasound received on the channels; using the acquired channel data to estimate coherence of the data and to derive dominance of an eigenvalue of a channel covariance matrix; and, based on the estimate and the derived dominance, distinguishing microcalcifications from background.

[0012] For such a device, a computer readable medium or alternatively a transitory, propagating signal is part of what is proposed herein. A computer program embodied within a computer readable medium as described below, or, alternatively, embodied within a transistory, propagating signal, has instructions executable by a processor for performing the acts of: using acquired channel data to estimate coherence of the data and to derive dominance of an eigenvalue of a channel covariance matrix; and, based on the estimate and the derived dominance, distinguishing microcalcifications from background.

[0013] Details of the novel, ultrasonic microcalcification identification technology are disclosed below with the aid of the following drawing, which is not drawn to scale, and the following formula sheet and flow charts.

BRIEF DESCRIPTION OF THE DRAWINGS

[0014] FIG. **1** is a schematic diagram of an ultrasonic microcalcification identification device in accordance with the present invention;

[0015] FIG. **2** is a set of exemplary mathematical definitions and relationships in accordance with the present invention; and

[0016] FIGS. **3**A-**3**D, **4**A-**4**C, and **5** are flow charts of an exemplary ultrasonic microcalcification identification process in accordance with the present invention.

DETAILED DESCRIPTION OF EMBODIMENTS

[0017] FIG. **1** depicts, by way of illustrative and non-limitative example, a medical ultrasound acquisition-data analysis device characterizable as an ultrasonic microcalcification identification device **100**.

[0018] The device **100** includes an ultrasound imaging probe **102** having an array **104** of transducer elements **106**. The probe **102** is shown as pressed into acoustic contact with breast tissue **107**.

[0019] The device **100** further includes channels **108** in connection with the elements **106**. The channels have respective sample delay elements **110**. The latter connect to a coherent summer **112**, the summer and the receive delay elements **110** together constituting a receive beamformer **114**. The delay elements **110** may be augmented to also provide amplitude weighting. Delay elements for steering and focusing transmit beams **116**, **118** can be implemented and are not shown. The multiple transmit beams **116**, **118** may be parallel, or may be differently angled, i.e., steered.

[0020] Also included in the device **100** are a coherence factor (CF) determination module **120**, an eigenvalue dominance determination module **122**, a microcalcification identification module **124**, a signal and image processor **126**, a display **128**, and a scanning controller **130**. The controller **130** controls the scanning as indicated by the oppositely-oriented scanning directional arrows **132**, **134** in FIG. **1**, and the other components of the device **100** shown in FIG. **1**.

[0021] The beamforming strategy for microcalcification detection is to involve channel-data-based parameters that favor point targets **136**, smaller than a spatial resolution, such as the lateral resolution **138** at that imaging depth **140**. Microcalcifications **142** resemble such targets **136** acoustically.

[0022] The microcalcification **142** is the dominant scatterer in its resolution cell and causes isotropic scattering. A coherence factor and an eigenvalue dominance criterion, both discussed herein below, are utilized to respectively assess the isotropic scattering and the dominance of the microcalcification. In the background tissue there is no such dominance of a single, isotropic scatterer.

[0023] Two parts of a bifurcated approach proposed herein accordingly are coherence estimation using multiple transmit beams and covariance matrix analysis to extract eigenvalues.

[0024] More generally, it is noted at the outset that channel data, after applying beamforming delays but before coherent summing, i.e., "post-delay channel data", **144** is outputted by the summer **112**. This is complex data generally in the form "a+bi", as shown in FIG. **1**, i.e., such that both the real and imaginary components of a datum can be nonzero. The channel data **144** is routed to the eigenvalue dominance determination module **122**. The same data **144** is routable to the CF module **120** for summing there, although summing can alternatively, or in addition, be performed in the summer **112** as seen from the alternative path **145** in FIG. **1**. Also, the beamforming done by the CF module **120** can stand alone in forming field points for further image processing in the signal and image processor **126**. Or, alternatively or in addition, summed output of the summer **112**, which may for example be subject, in the summer, to amplitude weighting, can be submitted for processing by the signal and image processor **126**. In either event, the signal and image processor **126** prepares the beamformed data for display, performing functions such as frequency compounding, logarithic compression and scan conversion.

[0025] Referring now to the first part of the bifurcated approach, coherence estimation, let S(m, n, tx, rx) denote complex RF channel data (or "delayed data") **144**, i.e., after applying beamforming delays and optionally amplitude weighting. Here, m is the imaging depth/time counter or index, n the channel index, tx the transmit beam index, and rx the receive beam index. A coherence factor (CF) or "focusing criterion" at a spatial point (m, rx), or field point, **146** with a single transmit beam **116** is:

$$CF_0(m, rx) \equiv \frac{\left|\sum_{n=1}^{N} S(m, n, rx, rx)\right|^2}{N\sum_{n=1}^{N}|S(m, n, rx, rx)|^2} = \frac{\left|\frac{1}{N}\sum_{n=1}^{N} S(m, n, rx, rx)\right|^2}{\frac{1}{N}\sum_{n=1}^{N}|S(m, n, rx, rx)|^2},$$

where N is the number of channels **108**. The term

$$\left|\frac{1}{N}\sum_{n=1}^{N} S(m, n, rx, rx)\right|^2$$

is denoted as I_c(m,rx), where the subscript "c" stands for coherent, as it can be interpreted as the average coherent intensity over channels at the point (m, rx). The denominator on the right can be expressed as

$$\frac{1}{N}\sum_{n=1}^{N}|S(m, n, rx, rx)|^2 = \frac{1}{N}\sum_{n=1}^{N}|\Delta S(m, n, rx, rx)|^2 + \left|\frac{1}{N}\sum_{n=1}^{N} S(m, n, rx, rx)\right|^2$$

where

$$\Delta S(m, n, rx, rx) = S(m, n, rx, rx) - \frac{1}{N}\sum_{n=1}^{N} S(m, n, rx, rx).$$

The term

$$\frac{1}{N}\sum_{n=1}^{N}|\Delta S(m, n, rx, rx)|^2$$

is denoted as I_{inc}(m, rx), where the subscript "inc" stands for incoherent. This is because I_{inc}(n, rx) reflects the average intensity of incoherent signals (in the surroundings of (m, rx) decided by the focusing quality on transmit) and is zero when the channel data **144** are fully coherent. Substituting terms,

$$CF_0(m, rx) = \frac{I_c(m, rx)}{I_{inc}(m, rx) + I_c(m, rx)} = \frac{1}{\frac{I_{inc}(m, rx)}{I_c(m, rx)} + 1}.$$

Therefore, CF_0(m, rx) indicates how much the point (m, rx) is brighter than its surroundings. CF_0 ranges between 0 and 1 and it reaches the maximum 1 if and only if the channel data **144** are fully coherent. Full coherence means that S(m, 1, rx, rx)=S(m, 2, rx, rx)= . . . =S(m, N, rx, rx). Around a strong point target or a reflector, the CF_0 value is high.

[0026] To distinguish point targets, which microcalcifications **142** in background tissue **148** resemble acoustically, from planar reflectors, multiple transmit beams **116**, **118** can be incorporated into CF estimation. CF is thereby redefinable as:

$$CF(m, rx) \equiv \frac{\sum_{tx=rx-\Delta}^{rx+\Delta}\left|\sum_{n=1}^{N} S(m, n, tx, rx)\right|^2}{\sum_{tx=rx-\Delta}^{rx+\Delta} N\sum_{n=1}^{N}|S(m, n, tx, rx)|^2} \quad \text{(definition 1)}$$

which definition, like the ones that follow, is repeated in FIG. **2**.

[0027] As mentioned above, the spatial point (m, rx) **146** is a function of both an associated receive beam rx **150** and a spatial depth **140** or time. The estimating operates on the delayed data **144** by summing, thereby performing beamforming. The CF(m, rx) estimate, or result of the estimating, **204** includes spatial compounding of the CF by summing, over multiple transmit beams **116**, **118**, a squared-magnitude function **206** and a squared beamsum **208**, i.e. summed result of beamforming. The function **206** and beamsum **208** are both formed by summing over the channels **108**.

[0028] Referring now to the second part the bifurcated approach, let R(m, rx) denote a covariance matrix, or "correlation/covariance matrix", **210** at the point (m, rx) obtained by temporal averaging over a range **214** of time or spatial depth **140**:

$$R(m, rx) \equiv \frac{1}{2d+1} \sum_{p=m-d}^{m+d} s(p, rx) s^H(p, rx) \quad \text{(definition 2)}$$

where

$$s(p, rx) = \begin{bmatrix} S(p, 1, rx, rx) \\ S(p, 2, rx, rx) \\ \vdots \\ S(p, N, rx, rx) \end{bmatrix}. \quad \text{(definition 3)}$$

As R(m, rx) is positive semidefinite, all of its eigenvalues **212** are real and nonnegative. Denote the eigenvalues by $\{y_i(m, rx)\}_{i=1}^{N}$ with $y_i \geq y_{i+1}$. Then the trace of R(m, rx) is

$$Tr\{R(m, rx)\} \equiv \sum_{i=1}^{N} R_{ii}(m, rx) = \sum_{i=1}^{N} \gamma_i(m, rx). \quad \text{(definition 4)}$$

The dominance **216** of the first eigenvalue **218** is represented as

$$ev_d(m, rx) \equiv \frac{1}{1 - \frac{\gamma_1(m, rx)}{Tr\{R(m, rx)\}}}. \quad \text{(definition 5)}$$

It is infinite if $y_i(m, rx)=0$ for $i \geq 2$ (i.e., if the rank of R(m, rx) is 1) as $Tr\{R(m, rx)\}=y_1(m, rx)$, and finite otherwise. Summing over several transmits **116**, **118** (beam averaging) could also be applied in correlation matrix analysis, as follows:

$$R(m, rx) \equiv \quad \text{(definition 6)}$$

$$\frac{1}{(2d+1)(2g+1)} \sum_{p=m-d}^{m+d} \sum_{tx=rx-g}^{rx+g} s(p, tx, rx) s^H(p, tx, rx)$$

-continued

where

$$s(p, tx, rx) = \begin{bmatrix} S(p, 1, tx, rx) \\ S(p, 2, tx, rx) \\ \vdots \\ S(p, N, tx, rx) \end{bmatrix} \quad \text{(definition 7)}$$

[0029] Another way of combining transmits is to form the covariance matrix from data generated by an algorithm that recreates focused transmit beams retrospectively. An example utilizing retrospective dynamic transmit (RDT) focusing is as follows, and, for other such algorithms such as plane wave imaging (see G. Montaldo, M. Tanter, J. Bercoff, N. Benech, and M. Fink, "Coherent plane-wave compounding for very high frame rate ultrasonography and transient elastography," IEEE Trans. Ultrason. Ferroelectr. Freq. Control, vol. 56, no. 3, pp. 489-506, 2009) and synthetic aperture beamforming (see J. A. Jensen, S. I. Nikolov, K. L. Gammelmark, and M. H. Pedersen, "Synthetic aperture ultrasound imaging," Ultrasonics, vol. 44, supplement, pp. e5e15, 2006), analogous eigenvalue dominance computations apply:

$$R(m, rx) \equiv \frac{1}{2d+1} \sum_{p=m-d}^{m+d} s_{RDT}(p, rx) s_{RDT}^H(p, rx)$$

where

$$s_{RDT}(p, rx) = \begin{bmatrix} S_{RDT}(p, 1, rx) \\ S_{RDT}(p, 2, rx) \\ \vdots \\ S_{RDT}(p, N, rx) \end{bmatrix},$$

and $S_{RDT}(p, n, rx)$ are the dynamically transmit-beamformed complex RF channel data obtained by performing retrospective dynamic transmit (RDT) focusing on the original channel data S(m, n, tx, rx). See U.S. Pat. No. 8,317,712 to Burcher et al., the entire disclosure of which is incorporated herein by reference.

[0030] In the above bifurcated approach, $CF_0(m, rx)$ or CF(m, rx) can, as with the dominance, likewise be obtained by temporal averaging over a range **214** of time or spatial depth **140**. Coherence factor can also be estimated using dynamically transmit-beamformed channel data as follows:

$$CF_{RDT}(m, rx) \equiv \frac{\left| \sum_{n=1}^{N} S_{RDT}(m, n, rx) \right|^2}{N \sum_{n=1}^{N} |S_{RDT}(m, n, rx)|2}.$$

[0031] According to J. R. Robert and M. Fink, "Green's function estimation in speckle using the decomposition of the time reversal operator: Application to aberration correction in medical imaging," J. Acoust. Soc. Am., vol. 123, no. 2, pp. 866-877, 2008, the dominance of the first eigenvalue $ev_d(m, rx)$ can be approximated by $1/(1-CF_1(m, rx))$, where $CF_1(m, rx)$ is a coherence factor obtained from channel data S(m, n, tx, rx). Temporal averaging **230**, averaging over

multiple transmit beams **116**, **118**, and/or RDT can be applied in calculating $CF_1(m, rx)$. Inversely, coherence factor can be approximated by eigenvalue dominance derived with proper averaging.

[0032] FIGS. **3**A-**3**D relate to the portion of the ultrasonic microcalcification identification process up until metric calculation. The procedure described below is an example of live, dynamic, real-time imaging, although it can be simplified to return a single B-mode image bearing the distinguished calcifications.

[0033] In accordance with a scanning process **302**, shown in FIG. **3**A, transmits **116**, **118** are issued (step S**302**). This can be done serially on transmit in a range around the center **152** of the receive beam **150** using for example RDT scanning sequences. For each transmit there can be multiple receive beams, leading to multiple transmits per receive beam. Or a single transmit **116** may be issued per receive beam **150** as is done for the estimating of $CF_0(m, rx)$, the estimate without beam averaging. In the case of a single transmit or in the case of multiple ones, for each transmit there is a receive, via the receive beam **150** (step S**304**) or there are multiple receives. The transmits **116** and receives **150** proceed, until scanning is complete or otherwise halted (step S**306**).

[0034] A concurrent channel data acquisition subprocess **304**, shown in FIG. **3**B, acquires complex channel data (step S**308**), and delays the data samples by channel (step S**310**). This occurs repeatedly, until scanning is complete or otherwise halted (step S**312**).

[0035] In a concurrent coherence factor estimation subprocess **306**, seen in FIG. **3**C, samples that vary by channel are obtained (step S**314**). They are coherently summed, thereby completing a beamforming procedure (step S**316**). The magnitude of each sample is calculated channel by channel (step S**318**). If there exists a next transmit **116**, for beam averaging, for the current spatial point **146** being interrogated (step S**320**), a transmit counter is incremented (step S**322**), and processing returns to the sample-obtaining step S**314**. Otherwise, if there does not exist a next transmit **116** (step S**320**), the transmit counter is reset (step S**324**). Summation for beamforming and summation of sample magnitudes are performed over all transmits **116** for the current spatial point **146** (step S**326**). The coherence factor CF **204** is computed (step S**328**).

[0036] Meanwhile, in a concurrent dominance derivation subprocess **308** of FIG. **3**D, samples are obtained that vary by channel (step S**330**). A conjugate transpose **220** of a column matrix of the samples ordered by channel is formed (step S**332**). A product **222** is taken of the two matrices (step S**334**). If a next transmit **116**, for beam averaging, exists for the current spatial point **146** (step S**336**), the transmit counter is incremented (step S**338**) and processing returns to the sample acquisition step S**330**. Otherwise, if a next transmit **116** does not exist (step S**336**), the transmit counter is reset (step S**340**). Query is then made as to whether a next neighbor point **224** for temporal averaging exists (step S**342**). If a next neighbor point **224** exists (step S**342**), the neighbor point counter is incremented (step S**346**) and processing returns to the sample acquisition step S**330**. Otherwise, if a next neighbor point **224** does not exist (step S**342**), the neighbor counter is reset (step S**348**). The product matrix from step S**334** is summed over the transmits **116** and neighbor points **224** (step S**350**). As seen from definition **2** in FIG. **2**, a covariance matrix with beam averaging **226** is computed based on the summed products **222** (step S**352**). A set of eigenvalues **212** are computed for the covariance matrix **226** by methods well known in the art (step S**354**). The largest **218** from among the eigenvalues is found (step S**356**). It is compared **228** with the set (step S**358**). The dominance **216** is calculated (step S**360**).

[0037] The estimation and derivation subprocesses **306**, **308** are executed in the context of scanning subprocess **402** which is presented in FIG. **4**A. In a first step, a metric is computed for the current spatial point **146** (step S**402**). Step S**402** corresponds to either the estimation or derivation subprocess **306**, **308**. Accordingly, both the coherence factor (CF) determination module **120** and the eigenvalue dominance determination module **122** invoke the instant scanning subprocess **402**. If time, rather than spatial depth, is being indexed for temporal tracking (step S**404**), and a next time exists for the current receive beam **150** (step S**406**), the time counter is incremented (step S**408**) and return is made to step S**402**. Likewise, if, instead of time, spatial depth is being indexed for temporal tracking (step S**404**), and a next spatial depth exists for the current receive beam **150** (step S**410**), the spatial depth counter is incremented (step S**414**) and return is made to step S**402**. If, on the other hand, no next time or spatial depth exists (steps S**406**, S**410**), correspondingly the time or spatial depth counter is reset (steps S**416**, S**418**). If, at this juncture, a next receive beam **150** exists in the current frame or scan (step S**420**), the receive beam counter is incremented (step S**422**). Otherwise, if no next receive beam **150** exists (step S**420**), the receive counter is reset (S**424**). If a next frame exists (step S**425**), processing points to the next frame (step S**426**) and return is made to the metric computation step S**402**.

[0038] The microcalcification identification module **124** concurrently executes a first version **404** of a microcalcification mapping subprocess, shown in FIG. **4**B. First, the CF **204** and the dominance **216** are combined, as by multiplication (step S**427**). If the product is large enough to meet a combination threshold (step S**428**), the respective (and current) spatial point **146** is added to the microcalcification map for the current imaging frame (step S**430**). A microcalcification **142** has therefore been distinguished from background **148**. If there is a next point in the frame (step S**432**), processing points to that next point (step S**434**) and return is made to the start of the subprocess **404**. Otherwise, if there is no next point in the current frame (step S**432**), but there is a next frame to process (step S**436**), processing points to the next point (step S**434**) and return is made to the start of the subprocess **404**.

[0039] Alternatively or in addition, the microcalcification identification module **124** concurrently executes a second version **406** of a microcalcification mapping subprocess, as seen from FIG. **4**C. If a first coherence threshold is met, i.e., the CF **204** is large enough to meet it (step S**440**), the current spatial point **146** is added to the microcalcification map for the current imaging frame (step S**442**). On the other hand, even if the first coherence threshold is not met (step S**440**), but the CF **204** is large enough to meet another, i.e., second, predetermined coherence threshold (step S**444**) and the dominance **216** is large enough to meet a dominance threshold (step S**446**), the current spatial point **146** is added to the microcalcification map (step S**442**). If a next point exists in the current frame (step S**448**), processing points to that next point (step S**450**) and return is made to step S**440**. If, on the other hand, with the first coherence threshold not being met

(step S440), if either the second coherence threshold or dominance threshold is likewise not met or both are not met (steps S444, S446), and if a next point exists (step S448), processing points to that next point (step S450) and return in made to step S440. In any event, when no next point in the current frame exists (step S448), if a next frame exists (step S452), processing points to that next frame (step S454) and return is made to step S440.

[0040] The microcalcification identification module 124 is also concurrently invoking a visual calcification discrimination subprocess 502, represented in FIG. 5. To the current frame for display, the corresponding microcalcification map is applied (step S502). All spatial points 146, e.g., voxels, in the current frame have been processed in either the first or second versions 404, 406 of the microcalcification mapping subprocess. The entries of the current microcalcification map denote microcalcifications 142 and are to be distinguished visually for presentation on-screen (step S504). This is done by highlighting, coloring or distinctive coloring, annotation with labels and/or screen pointers, etc., and is done by means of overlays, the adjustment of grey level, or any other known and suitable means. The image bearing the distinguished calcifications is displayed (step S506). If a next frame exists (step S508), processing points to that next frame (step S510), and returns to the map application step S502.

[0041] A medical ultrasound acquisition-data analysis device acquires channel data via ultrasound received on the channels, uses the acquired channel data to estimate data coherence and derive dominance of an eigenvalue of a channel covariance matrix and, based on the estimate and dominance, distinguishes microcalcifications from background. Microcalcifications may then be made distinguishable visually onscreen via highlighting, coloring, annotation, etc. The channel data operable upon by the estimating may have been subject to beamforming delays and may be summed in a beamforming procedure executed in the estimating. In the estimating and deriving, both field point-by-field point, multiple serial transmits may be used for each field point. In one embodiment results of the estimating and deriving are multiplied point-by-point and submitted to thresholding.

[0042] While the invention has been illustrated and described in detail in the drawings and foregoing description, such illustration and description are to be considered illustrative or exemplary and not restrictive; the invention is not limited to the disclosed embodiments.

[0043] For example, within the intended scope of what is proposed herein is a computer readable medium, as described below, such as an integrated circuit that embodies a computer program having instructions executable for performing the subprocesses 306, 308, 404, 406, 502 described above for microcalcification discrimination. The functions are implementable by any combination of software, hardware and firmware.

[0044] Other variations to the disclosed embodiments can be understood and effected by those skilled in the art in practicing the claimed invention, from a study of the drawings, the disclosure, and the appended claims. In the claims, the word "comprising" does not exclude other elements or steps, and the indefinite article "a" or "an" does not exclude a plurality. Any reference signs in the claims should not be construed as limiting the scope.

[0045] A computer program can be stored momentarily, temporarily or for a longer period of time on a suitable computer-readable medium, such as an optical storage medium or a solid-state medium. Such a medium is non-transitory only in the sense of not being a transitory, propagating signal, but includes other forms of computer-readable media such as register memory, processor cache, RAM and other volatile memory.

[0046] A single processor or other unit may fulfill the functions of several items recited in the claims. The mere fact that certain measures are recited in mutually different dependent claims does not indicate that a combination of these measures cannot be used to advantage.

1. A medical ultrasound acquisition-data analysis device having a plurality of channels and configured for:

acquiring channel data via ultrasound received on the channels;

wherein the acquired channel data are used to estimate coherence of said data and to derive dominance of an eigenvalue of a channel covariance matrix; and,

based on the estimate and the derived dominance, distinguishing microcalcifications from background.

2. The device of claim 1, comprising a display and further configured for displaying, on said display, the distinguished microcalcifications in an ultrasound view.

3. The device of claim 2, further configured for displaying on said display, said microcalcifications in a presentation that, based on a result of said distinguishing, visually discriminates said microcalcifications from said background.

4. The device of claim 1, said using comprising using said data to estimate coherence of said data individually with respect to a plurality of spatial points having respectively both a) an associated receive beam; and b) a spatial depth or time.

5. The device of claim 4, said using further comprising using said channel data in the deriving separately by point with respect to the plural points.

6. The device of claim 4, further configured for combining the estimates and the derivations point-by-point for said plurality of points.

7. The device of claim 6, said combining comprising multiplying said estimates by said derivations point-by-point for said plurality of points.

8. The device of claim 6, said combining yielding respective values, said device being further configured for thresholding said values, output of said thresholding spatially identifying said microcalcifications.

9. The device of claim 1, said estimating comprising spatial compounding of a 1 coherence factor by summing, over multiple transmit beams, a function of said data with respect to: a) a given receive beam; and b) a given spatial depth or time.

10. The device of claim 9, said estimating further comprising summing said function over said channels.

11. The device of claim 1, further configured for a datum from among said acquired channel data being complex, with its real and imaginary parts both being nonzero, upon use for the estimating and for the deriving, said data, upon said use, having been subject to beamforming delay.

12. The device of claim 1, said using comprising subjecting the acquired channel data to beamforming delays.

13. The device of claim **12**, said device being further configured such that the estimating operates on the delayed data by summing, thereby performing beamforming.

14. The device of claim **12**, said device being further configured such that the deriving operates on the delayed data separately by channel.

15. The device of claim **1**, said matrix having a plurality of eigenvalues, said eigenvalue being among the plural eigenvalues, said dominance being a metric representing a comparison between said eigenvalue and said plural eigenvalues, said device being configured for creating said matrix from said acquired channel data, said deriving comprising computing said eigenvalue.

16. The device of claim **1**, said channel data being, upon said deriving, complex radiofrequency channel data to which beamforming delays have been applied, said deriving comprising taking a conjugate transpose of a matrix of said channel data, entries of said conjugate transpose varying by channel.

17. The device of claim **16**, said deriving comprising:

forming a product matrix, said forming comprising multiplying said matrix of said channel data by said conjugate transpose; and

averaging said product matrix over a range of spatial depth or time to derive said dominance corresponding to a given spatial point.

18. The device of claim **16**, said deriving comprising:

forming a product matrix, said forming comprising multiplying said matrix of said channel data by said conjugate transpose; and

averaging said product matrix over multiple transmits.

19. The device of claim **16**, configured for, in creating said complex radiofrequency channel data, using an algorithm that recreates focused transmit beams retrospectively.

20. The device of claim **1**, said distinguishing comprising deciding, based on application of a coherence threshold to a result of the estimating, that a microcalcification resides at a given spatial point.

21. The device of claim **20**, said distinguishing comprising checking, if the decision is other than that a microcalcification resides at the given spatial point, whether said result and said derived dominance respectively meet another coherence threshold and a dominance threshold.

22. The device of claim **1**, said acquiring for a microcalcification particle **1** being performed with a spatial resolution, said particle being smaller than said resolution.

23. The device of claim **1**, said background being body tissue which said microcalcifications reside.

24. A computer readable medium embodying a program for medical ultrasound acquisition-data analysis, said program having instructions executable by a processor for performing a plurality of acts, among said plurality there being the acts of:

acquiring channel data via ultrasound received on multiple channels;

using the acquired channel data to estimate coherence of said data and to derive dominance of an eigenvalue of a channel covariance matrix; and,

based on the estimate and the derived dominance, distinguishing microcalcifications from background.

* * * * *

专利名称(译)	用于超声微钙化检测的波束形成技术		
公开(公告)号	US20160296202A1	公开(公告)日	2016-10-13
申请号	US14/777564	申请日	2014-03-12
[标]申请(专利权)人(译)	皇家飞利浦电子股份有限公司		
申请(专利权)人(译)	皇家飞利浦N.V.		
当前申请(专利权)人(译)	皇家飞利浦N.V.		
[标]发明人	ROBERT JEAN LUC HUANG SHENG WEN RADULESCU EMIL GEORGE VIGNON FRANCOIS GUY GERARD MARIE ERKAMP RAMON QUIDO		
发明人	ROBERT, JEAN-LUC HUANG, SHENG-WEN RADULESCU, EMIL GEORGE VIGNON, FRANCOIS GUY GERARD MARIE ERKAMP, RAMON QUIDO		
IPC分类号	A61B8/08 A61B8/00		
CPC分类号	A61B8/085 A61B8/461 A61B8/5207 A61B8/0825 A61B8/5223		
优先权	61/803634 2013-03-20 US 61/907022 2013-11-21 US		
其他公开文献	US10357224		
外部链接	Espacenet USPTO		

摘要(译)

医学超声采集数据分析设备通过在信道上接收的超声获取信道数据（144），使用所获取的信道数据来估计数据一致性并导出信道协方差矩阵的特征值的优势并且，基于估计和优势，将微钙化（142）与背景区分开来。然后可以通过突出显示，着色，注释等在屏幕上可视地区分微钙化。可以通过估计操作的信道数据可以经历波束形成延迟并且可以在估计中执行的波束形成过程中求和。在估计和推导中，两个场逐点，多个串行发送（116,118）可以用于每个场点。在一个实施例中，估计和导出的结果逐点相乘并提交给阈值处理。